Highly time-resolved measurements of element concentrations in PM₁₀ and PM₂.₅: Comparison of Delhi, Beijing, London, and Krakow

Pragati Rai[1], Jay G. Slowik[1], Markus Furger[1], Imad El Haddad[1], Suzanne Visser[2], Yandong Tong[1], Atinderpal Singh[3], Günther Wehrle[1], Varun Kumar[1], Anna K. Tobler[1], Deepika Bhattu[1,a], Liwei Wang[1], Dilip Ganguly[4], Neeraj Rastogi[3], Ru-Jin Huang[5], Jaroslaw Necki[6], Junji Cao[5], Sachchida N. Tripathi[7], Urs Baltensperger[1], André S. H. Prévôt[1]

[1]Laboratory of Atmospheric Chemistry, Paul Scherrer Institute, Forschungsstrasse 111, 5232 Villigen PSI, Switzerland
[2]Centre for Environmental Quality, National Institute for Public Health and the Environment, 3720 BA, Bilthoven, the Netherlands
[3]Geosciences Division, Physical Research Laboratory, Ahmedabad 380009, India
[4]Centre for Atmospheric Sciences, Indian Institute of Technology Delhi, New Delhi 110016, India
[5]Key Laboratory of Aerosol Chemistry and Physics, Institute of Earth Environment, Chinese Academy of Sciences, Xi'an 710075, China
[6]Faculty of Physics and Applied Computer Science, Department of Applied Nuclear Physics, AGH University of Science and Technology, 30059 Krakow, Poland
[7]Department of Civil Engineering and Department of Earth Sciences, Indian Institute of Technology Kanpur, Kanpur, Uttar Pradesh 208016, India
[a]now at: Department of Civil and Infrastructure Engineering, Indian Institute of Technology Jodhpur, Jodhpur, Rajasthan 342037, India

Correspondence to: Markus Furger (markus.furger@psi.ch), André S. H. Prévôt (andre.prevot@psi.ch), S. N. Tripathi (snt@iitk.ac.in), Junji Cao (cao@loess.llqg.ac.cn), Jaroslaw Necki (necki@agh.edu.pl)

Abstract. We present highly time-resolved (30 to 120 min) measurements of size-fractionated (PM₁₀ and PM₂.₅) elements in two cities in Asia (Delhi and Beijing) and Europe (Krakow and London). For most elements, the mean concentrations in PM₁₀ and PM₂.₅ are higher in the Asian cities (up to 24 and 28 times, respectively) than in Krakow, and often higher in Delhi than in Beijing. Among European cities, Krakow shows higher elemental concentrations (up to 20 and 27 times, respectively) than London. Hourly maximum concentrations of Pb and Zn reach up to 1 µg m⁻³ in Delhi, substantially higher than at the other sites. The enrichment factor of an element together with the size distribution allows for a rough classification of elements by major sources. We define five groups: (1) dust-related, (2) non-exhaust traffic emissions, (3) solid fuel combustion, (4) mixed traffic/industrial emissions, and (5) industrial/coal/waste burning emissions, with the last group exhibiting the most site-to-site variability. We demonstrate that the high time resolution and size-segregated elemental dataset can be a powerful tool to assess aerosol composition and sources in urban environments. Our results highlight the need to consider the size distributions of toxic elements, diurnal patterns of targeted emissions, and local vs. regional effects in formulating effective environmental policies to protect public health.

1 Introduction

The percentage of the global population living in urban areas with more than 1 million inhabitants has been steadily increasing over the last decades (Krzyzanowski et al., 2014). Air pollution in these cities is a major contributor to the global disease burden (Lim et al., 2012), with more than 96% of the population in these cities exposed to PM₂.₅ (particulate matter with an aerodynamic diameter below 2.5 µm) concentration above World Health Organization (WHO) air quality standards (Krzyzanowski et al., 2014). Smaller particles are likely more toxic since they can penetrate deep into the lungs (Miller et al., 1979). Particle toxicity depends also on PM composition (Kelly and Fussell, 2012), with identified toxic constituents including elemental and organic carbon, and metals. Transition metals such as Fe, V, Ni, Cr^{VI}, Cu and Zn are of particular concern due to their potential to produce reactive oxygen species (ROS) in biological tissue (Manke et al., 2013). Moreover, metals such as Pb, Cd and the metalloid As accumulate in body tissue and contribute to many adverse health effects, such as lung cancer,

1

cognitive deficits, and hearing impairment (Jaishankar et al., 2014). Elements are also recognized as effective markers for source apportionment (SA), especially for anthropogenic emissions in urban areas (e.g., traffic, industry and power production). Emissions from these sources vary on timescales of a few hours or less, and such rapid changes cannot be resolved by conventional 24-h filter measurements. The vast majority of elemental SA studies in the literature are limited by the time resolution of the input samples (Dall'Osto et al., 2013; Pant and Harrison, 2012). Highly time-resolved and size-segregated measurements are thus required for the determination of elemental PM sources and health effects within urban areas under varying meteorological conditions.

Efforts in European and Asian countries to tackle poor air quality include the EURO norms (EEA, 2018) in European cities to control vehicular emissions, odd-even traffic regulations in Delhi (Kumar et al., 2017) and Beijing (An et al., 2019), and the "stop smog" program in Poland (Shah, 2018). In addition, strict emission control measures were implemented in China (Gao et al., 2016) in September 2013, by lowering the fraction of coal in energy production from 24 % in 2012 to 10 % in 2017. Evaluation and optimization of such programs require elucidation of the sources and processes governing PM abundance and composition. This remains challenging and may strongly differ from site to site depending on local environmental conditions. To assess this, we present high time resolution PM_{10} and $PM_{2.5}$ metal and trace element concentrations in four Asian and European cities: Delhi, Beijing, Krakow, and London. A simple conceptual framework allows characterization of major sources, site-to-site similarities and local differences, and identification of key information required for efficient policy development. Moreover, when the aim of the analysis is not to obtain quantitative information, this method is proved particularly useful since it does not require a full SA analysis (presented elsewhere for London and Delhi (Visser et al., 2015a; Rai et al., 2020)), which is complex and time-consuming, and which can be challenging to compare across sites due to differences in source definitions.

2 Materials and Methods

2.1 Description of the sampling sites

The sampling site (40.00° N, 116.38° E) in Beijing was located in a residential area north of the urban core, near the Olympic Park without any nearby industrial sources. It is a typical urban site in the central zone of Beijing. It is located approximately 1.2 km away from the west 3rd Ring Road and 2.7 km away from the north 2nd Ring Road. Both ring roads are characterized by heavy traffic. Coal-based heating is a major sector of coal consumption in Northern China (Tian et al., 2015). The measurements were performed from 6 November to 12 December 2017.

The sampling site (50.06° N, 19.91° E) in Krakow was located in a residential area close to the city center. The major local sources of pollution are municipal emissions, combustion, industry, and traffic. Traffic in the city is dense with frequent traffic jams (~1 km away from sampling location). Factories (steel and non-ferrous metallurgical industries) are located at a distance of about 10 km from the sampling site. Additionally, a coal power plant is located in the southern area of the city. Moreover, a zinc ore industry is situated about 50 km to the north of the city. The sources with the highest PM emission rates are situated in the northeastern part of Krakow, i.e., Huta Arcelor Mittal steel works, the Cementownia cement factory and the EC Krakow coal-fired power plant (Junninen et al., 2009). However, in Krakow, there are numerous small coal-fired low-efficiency boilers (LE-boilers) distributed over the city. The measurements were performed from 11 to 23 October 2018. It is important to note that the sampling period in Krakow is different from the rest of the sites.

The Delhi sampling location (28.54° N, 77.19° E) was situated in a residential and commercial area in the south part of Delhi. Roads with heavy traffic within 2-5 km surround the sampling location in all directions. Many anthropogenic sources such as traffic, agricultural residue burning, waste burning, one coal based power plant, various micro-, small-, and medium-scale manufacturing and processing units such as metal processing, electroplating, and paint and chemical manufacturing for pre-treatment of metals, might contribute to the low air quality of this region. However, the coal based power plant in the southeast

direction (18 km) was shut down in October 2018, although evacuation of fly ash continued during the study period. The measurements were performed from 15 January to 9 February 2019.

The London sampling location (51.52° N, 0.21° W) classified as urban background, was within a school ground in a residential area of North Kensington (NK). Long-term measurements of air pollutants at NK have been described in detail in a previous study (Bigi and Harrison, 2010), and are considered as representative of the background air quality for most of London. NK is situated within a heavy traffic suburban area of London. The measurements were performed from 6 January to 11 February 2012.

2.2 Instrumentation

In Beijing, Delhi, and Krakow, sampling and analysis was conducted with an Xact 625i® Ambient Metals Monitor (Cooper Environmental, Tigard, OR, USA) with an alternating PM_{10} and $PM_{2.5}$ inlet switching system (Furger et al., 2020). Details of the Xact can be found in previous studies (Cooper et al., 2010; Furger et al., 2017; Rai et al., 2020; Tremper et al., 2018). The field measurements with the Xact were performed with 1 h time resolution in Beijing and 0.5 h time resolution in Krakow and Delhi. The instrument was able to detect 34 elements (Al, Si, P, S, Cl, K, Ca, Ti, V, Cr, Mn, Fe, Co, Ni, Cu, Zn, Ga, Ge, As, Se, Br, Rb, Sr, Y, Zr, Cd, In, Sn, Sb, Ba, Hg, Tl, Pb and Bi). However, some of the elements were below minimum detection limit (MDL) of the instrument (Table S1) for certain periods of time. Therefore, we discarded the elements that were below MDL in PM_{10} and $PM_{2.5} \geq 80\%$ of the time.

In London, we deployed a rotating drum impactor (RDI) which sampled with 2 h time resolution in size-segregated stages: $PM_{10–2.5}$ (coarse), $PM_{2.5–1.0}$ (intermediate) and $PM_{1.0–0.3}$ (fine). Trace element composition of the RDI samples was determined by synchrotron radiation-induced X-ray fluorescence spectrometry (SR-XRF) at the X05DA beamline (Flechsig et al., 2009) at the Swiss Light Source (SLS), Paul Scherrer Institute (PSI), Villigen PSI, Switzerland, and at Beamline L at the Hamburger Synchrotronstrahlungslabor (HASYLAB), Deutsches Elektronen-Synchrotron (DESY), Hamburg, Germany (beamline dismantled in November 2012). In total 25 elements were quantified (Na, Mg, Al, Si, P, S, Cl, K, Ca, Ti, V, Cr, Mn, Fe, Ni, Cu, Zn, Br, Sr, Zr, Mo, Sn, Sb, Ba, Pb). Details of the RDI-SR-XRF analysis were described in previous studies (Bukowiecki et al., 2008; Richard et al., 2010; Visser et al., 2015b). Due to the RDI's omission of particles smaller than 300 nm, the fine mode elemental data for London is less reliable as compared to the other sites. While the comparison of size-resolved London data with the other sites should therefore be interpreted with caution, we present London $PM_{2.5}/PM_{10}$ ratios, group classification (in PM_{10} and $PM_{2.5}$) and their diurnal patterns (in $PM_{2.5}$ and coarse (PM_{10}-$PM_{2.5}$)) in the Supplement (Figs. S4, S5 and S8, respectively).

Xact measurements of Cl and S were compared to the chloride and sulfate data obtained from co-located aerosol mass spectrometer (AMS) measurements (Fig. S1). The AMS instruments consisted of a high-resolution long-time-of-flight (L-TOF) AMS deployed for online measurements of size segregated mass spectra of non-refractory (NR)-$PM_{2.5}$ with 2 min resolution in Beijing and a HR-TOF-AMS of NR-PM_1 with 2 min resolution in Delhi. The scatter plots exhibit a good correlation, which is reflected by a Pearson's R of 0.91 (Delhi) and 0.96 (Beijing) for S vs sulfate, and 0.98 (Delhi) and 0.97 (Beijing) for Cl vs chloride. The correlation resulted in a slope of 1.13 (Delhi) and 1.23 (Beijing) for sulfate, and 1.03 (Delhi) and 1.9 (Beijing) for Cl. The S measurements of the two instruments agree within the typical uncertainties of such measurements (~25%) (Canagaratna et al., 2007; Furger et al., 2017). In addition, the Delhi measurements cover different size fractions ($PM_{2.5}$ for the Xact vs. PM_1 for the AMS).

The Xact/AMS ratio for Cl observed in Beijing likely occurs because the relative ionization efficiency for AMS measurements of Cl was not determined in Beijing (whereas calibrations with NH_4Cl were performed in Delhi). In addition, the Beijing measurements likely have a higher fraction of other forms of Cl (e.g., $ZnCl_2$, $PbCl_2$, $FeCl_3$), which are not efficiently detected in standard AMS operation. High Cl concentrations from November to March in Beijing are reported in previous studies, which is believed to be associated with coal burning (Yao et al., 2002; Zhang et al., 2019). The contribution from sea-salt

particles is less important because the sampling site in Beijing is about 200 km from the sea. However, the sea/road-salt discussion would be strengthened by the measurement of Na, which is an important tracer of sea/road-salt in the form of NaCl. While Na and Cl are good tracers for sea/road-salt, the Cl/Na ratio in Beijing during winter is reported to be much higher (2.3) than the ratio in seawater (1.17) (Yao et al., 2002).

2.3 Crustal enrichment factor (EF) analysis

EF analysis was applied to determine the enrichment of a given element relative to its abundance in the upper continental crust (UCC). For this analysis Ti (Fomba et al., 2013; Majewski and Rogula-Kozłowska, 2016; Wei et al., 1999) was selected as the reference element due to its stable and spatially homogenous characteristics in the soil. The compilation of UCC (Rudnik and Gao, 2003) was used to calculate EFs and crustal contributions on elemental concentrations. For an element (X) in a sample, the EF relative to Ti is given as:

$$EF = \frac{(X/Ti)_{Sample}}{(X/Ti)_{Crust}} \tag{1}$$

The unexpectedly low EFs observed for Si (0.41–0.45) and compared to previous studies (Majewski and Rogula-Kozłowska, 2016; Tao et al., 2013), are likely due to self-attenuation issues in XRF analysis for lighter elements (atomic number<19), which may cause underestimation in their concentrations (Maenhaut et al., 2011; Visser et al., 2015b). Therefore, the measurements of Al and Si from Xact need to be treated with caution. However, low EFs for Si is also probably due to crust-air fractionation in the wind-blown generation of crustal aerosol particles (Rahn, 1976). Given that Si is the only outlier across all measured elements, a major anthropogenic contribution to Ti seems unlikely. However, Ti emission is possible from non-exhaust traffic sources, measured in road dust samples worldwide (Amato et al., 2009; Pant et al., 2015).

3 Results

3.1 PM$_{10el}$ and PM$_{2.5el}$ concentration

Hourly average elemental PM$_{10}$ (PM$_{10el}$) and elemental PM$_{2.5}$ (PM$_{2.5el}$) concentrations were measured, where Figure 1 (a, b) summarizes the results of 18 elements measured at all four sites. Total measured concentrations at Delhi (54 µg m^{-3} in PM$_{10}$; 32 µg m^{-3} in PM$_{2.5}$) are three times higher than those at the other sites, followed by Beijing (16.7 µg m^{-3}; 5.2 µg m^{-3}), Krakow (9 µg m^{-3}; 4.3 µg m^{-3}) and London (1.9 µg m^{-3}; 0.9 µg m^{-3}) (see Fig. S2a for average value statistics). Although the measurement periods do not overlap, they were all performed during the colder months of the year (partially true for Krakow, see Section 2.1), and characteristic features of each site are evident. For the four sites PM$_{10el}$ diurnal cycles, and PM$_{10el}$ and PM$_{2.5el}$ time series, are shown in Fig. 4 and S2b, respectively. The total PM$_{10el}$ and PM$_{2.5el}$ concentrations in Delhi show a strong diurnal cycle, with high concentrations overnight and in the early morning hours, followed by a sharp decrease during the day (Fig. 4 and Fig. S2b). In contrast, Beijing experiences multi-day haze events with only minor diurnal cycling (Fig. S3). In Krakow and London, concentrations are mostly elevated during the rush-hours and during daytime in general (from 08:00 until 18:00 local time (LT)).

At all four sites, Si, Cl, Fe, S, Ca, and K account for >95% of PM$_{10}$ (>88% without K) and >94% of PM$_{2.5}$ (see Fig. 1b, Tables S2 and S3). Among elements with higher atomic numbers (Z= 29–82), Zn and Pb are highest at all sites except London (where Zn and Cu show the highest concentrations). Figure 1d presents the mean PM$_{10el}$ concentrations normalized to those in Krakow. With rare exceptions, element concentrations were highest in Delhi followed by Beijing, Krakow, and London. The concentrations of toxic PM$_{10el}$ (Cr, Ni, Fe, Cu, Zn, As and Pb) in Delhi are higher than at any other site, such as Cr (2 to 9 times), Ni (2 to 8 times), Mn (1 to 16 times), Cu (4 to 13 times), Zn (5 to 95 times) and Pb (12 to 205 times). However, the mean concentrations of carcinogenic elements (Pb, Ni, As, and Cr) (IARC, 2020) fall below the US EPA recommended inhalation reference concentrations (RfC) for resident air (200 ng m^{-3}, 20 ng m^{-3}, 15 ng m^{-3}, and 100 ng m^{-3}, respectively)

(USEPA, 2020) except for Pb in Delhi, which exceeds the RfC by more than a factor of 2. Individual exceedances of the RfC are relatively common in Delhi for Pb (52.8% of data) and As (34%), indicating severe risks to human health. At other sites, RfC exceedances are less common, comprising only 10% of As data in Beijing, and 1.76% of Cr and 1.4% of Ni in Krakow; no other RfC exceedances are observed.

3.2 Characteristic element groups

To evaluate the similarities and differences in element behavior across sites, we investigate the PM_{10} EF for each element, where EFs >> 1 indicate strong anthropogenic influence, and their corresponding $PM_{2.5}$ to PM_{10} ratios. The mass ratio $PM_{2.5}/PM_{10}$ for an element gives rough indication of the particle size distribution that reflects the corresponding emission processes and can provide insight into specific sources. For example, abrasion processes (e.g., mineral dust resuspension and brake/tire wear) result in coarse particles, whereas combustion and industrial processes are more likely to emit fine particles. Figure 2 shows the PM_{10} EFs as a function of $PM_{2.5}/PM_{10}$ for all elements measured at Delhi, Beijing, and Krakow (see Fig. S5 for London). Each site is shown separately in Fig. 2 and overlaid in Fig. S5. PM_{10} EFs for all sites and $PM_{2.5}/PM_{10}$ for Delhi, Beijing, and Krakow are shown in Fig. 1c and Fig. 3 (see Fig. S4 for London together with other sites), respectively. In general, EFs increase with increasing $PM_{2.5}/PM_{10}$. From Fig. 2, we divide the measured elements into 5 groups based on their position in the EF vs. $PM_{2.5}/PM_{10}$ space; this framework provides insight into element sources and emission characteristics. The classification for London is uncertain due to the lower cut-off issue mentioned in Section 2.2, but some qualitative agreement with the other sites is evident, with the largest differences related to the $PM_{2.5}/PM_{10}$ ratio. Therefore, London is included in the group classification below, although the data are shown in the Supplement for ease of viewing. Figure 4 compares the PM_{10} diurnal cycles of representative elements from the five groups for all four sites normalized to the mean element concentration, while Fig. 5 compares the absolute concentrations of $PM_{2.5}$ and coarse diurnals for the same elements on a site-by-site basis for Delhi, Beijing and Krakow (See Fig. S8 for London). Diurnals of other elements are shown in Figs. S6 and S7. The groups are discussed below.

Group 1 consists of elements with the lowest EFs and the highest fraction of coarse particles. It includes Ca, Si, and Ti at all three sites, Sr at Delhi and Beijing, Fe in Delhi, and Zr in Beijing. Elements associated with this group are typically of crustal origin, consistent with their position in Fig. 2. In contrast, Zr and Fe have been linked to both brake wear and mineral dust in urban environments (Moreno et al., 2013; Visser et al., 2015b).

Si is selected as the Group 1 representative element. A strong traffic influence (i.e., rush-hour peaks) on PM_{10} is evident at London, Krakow, and Delhi, while a much flatter diurnal pattern with only small rush-hour effects is evident in Beijing (Fig. 4). $PM_{2.5}$ concentrations are very low and in general not significant relative to PM_{10} (Fig. 5). These diurnal patterns are consistent with vehicle-induced resuspension of the dust deposited on the road surface, which in turn derive mostly from road abrasion, vehicle abrasion and airborne dust from construction activities or agricultural soil (Thorpe and Harrison, 2008 and references therein).

Group 2 elements have low EF but mean $PM_{2.5}/PM_{10}$ between 0.22 and 0.43. The increased $PM_{2.5}/PM_{10}$ value also corresponds to increased temporal variation in $PM_{2.5}/PM_{10}$, as shown by the larger interquartile range in Fig. 3. Group 2 includes Ba, Ni, Mn at all three sites, while Rb, Cr, Fe, and Zr at two sites, and Sr at a single site (Fig. 2). Several of these elements are associated with multiple sources, including coarse traffic emissions such as brake wear (e.g., Ni, Mn, Fe, Ba and Zr) (Bukowiecki et al., 2010; Srimuruganandam and Nagendra, 2012; Visser, et al., 2015a) and other anthropogenic sources such as industrial emissions or oil burning (Ni), or crustal material (Fe and Zr).

Because of these multiple sources, several Group 2 elements show significant site-to-site variation, despite remaining in or near the group boundaries. For example, Fig. 3 shows that Ni has a similar lower quartile for $PM_{2.5}/PM_{10}$ across all sites, while the upper quartile is much higher at Krakow. This is likely due to the strong influence of local steel/non-ferrous metallurgical industries (Samek et al., 2017a; Samek et al., 2017b), whereas the other sites are more strongly influenced by non-exhaust

5

emissions and dust (Grigoratos and Martini, 2015; Pant and Harrison, 2012; Yu, 2013). Such differences are also evident in the Ni diurnals and time series (Figs. S6, S7 and S9), as Ni concentrations in Krakow are driven by strong isolated plumes.

210   As an example of a typical Group 2 element, the diurnal patterns of Ba are shown in Figs. 4, 5 and S8. Similar to Group 1, significant rush-hour peaks are evident, although the trend is now also reflected in $PM_{2.5}$. In the Asian cities, high concentrations are also observed overnight. This is likely related to heavy-duty vehicular activities, which in these cities occur predominantly at night due to their ban during peak traffic hours (07:30 – 11:00 LT and 17:00 – 22:00 LT and less dominant during daytime) in Delhi (Rai et al., 2020) and the entire day in Beijing (Zheng et al., 2015). As both non-exhaust traffic

215   emissions (i.e., brake wear and dust resuspension) are related to traffic activity, the time series of most elements in Groups 1 and 2 are relatively well correlated, although not as tightly as the Group 1 elements are among themselves due to their common source. This is illustrated in the correlation matrices shown in Fig. S10, where elements are sorted by group along each axis. Group 2 elements are also relatively well correlated among themselves at all sites, with the exception of Ni at Krakow for the reasons discussed above.

220   **Group 3** includes K at all three sites and adds Rb at Krakow (Fig. 2). These elements show low EF and high $PM_{2.5}/PM_{10}$, although uncertainties are high for Rb at Krakow given that 86% and 65% data points in $PM_{2.5}$ and PM_{10}, respectively, are below MDL. Although coarse mode K can result from sea/road salt (Gupta et al., 2012; Zhao et al., 2015) and mineral/road dust (Rahman et al., 2011; Rogula-Kozłowska, 2016; Viana et al., 2008), the high fraction of K observed in the fine mode suggests solid fuel (coal and wood) burning as a larger source (Cheng et al., 2015; Pant and Harrison, 2012; Rogula-Kozłowska,

225   et al., 2012; Rogula-Kozłowska, 2016; Viana et al., 2013; Waked et al., 2014). Further, Delhi, Beijing and Krakow are far from the ocean and de-icing salt was not used on the roads during the measurement periods. In London and Delhi, K was attributed to solid fuel combustion via SA studies (Rai et al., 2020; Visser et al., 2015a). The diurnals in Delhi and Krakow show elevated values in the evening (Fig. 4), which is likewise consistent with solid fuel combustion for domestic heating. However, in Beijing only $PM_{2.5}$ exhibits such a diurnal variation (Fig. 5), whereas the PM_{10} fraction is similar to the other sites

230   without a clear diurnal variation (Fig. 4). This corresponds to a wider spread of $PM_{2.5}/PM_{10}$ at Beijing (with the lower quartile approaching values typical of Group 1), suggesting a larger contribution from dust.

       Group 4 has somewhat higher EFs than Groups 1-3 and moderate $PM_{2.5}/PM_{10}$. The group contains Cu at Beijing and Krakow, as well as Sn at Beijing and Cr at Krakow. No elements are assigned to this group in Delhi, although Cu is near the border. The EFs of these elements are >> 100 in $PM_{2.5}$ and > 10 in PM_{10} (Fig. S5), indicating strong anthropogenic influence. The

235   Group 4 elements are typically emitted from both traffic (characteristic of Group 2) and industrial or waste combustion sources (Group 5), and their position in Fig. 2 reflects the combination of these different sources. For example, Cu derives from brake wear in Europe (Thorpe and Harrison, 2008; Visser et al., 2015a) and Asia (Iijima et al., 2007), while Cu and Sn are also emitted from industry or waste burning (Chang et al., 2018; Das et al., 2015; Fomba et al., 2014; Kumar et al., 2015; Venter et al., 2017). Cr has also been found in the emissions from both traffic (Hjortenkrans et al., 2007; Thorpe and Harrison, 2008)

240   and oil burning in Krakow (Samek et al., 2017a).

       The diurnal patterns of Cu are shown in Figs. 4, 5 and S8. London, Beijing, and Krakow all show peaks during the morning and evening rush-hours, mainly due to the PM_{10} fraction. In Krakow, $PM_{2.5}$ is approximately correlated with the coarse fraction, although the morning peak appears ~2 h later, while in Beijing $PM_{2.5}$ Cu is instead elevated at night. Delhi contrasts sharply with the other sites, which probably is the reason why Cu in Delhi is not categorized in Group 4. Figure 3 shows that the

245    $PM_{2.5}/PM_{10}$ medians and quartiles are similar, but the mean (0.72 in Delhi, and 0.46 in Beijing and Krakow) is substantially higher in Delhi because the Cu time series (Fig. S11) is subject to a series of high intensity $PM_{2.5}$ plumes from local industries and/or waste burning. These plumes are tightly correlated with those of Cd, suggesting emissions from Cd-copper alloy manufacturing plants (Vincent and Passant, 2006), electronic waste burning (Rai et al., 2020; Owoade et al., 2015) and/or steel metallurgy (Tauler et al., 2009).

250 **Group 5** elements have both the highest EF and highest $PM_{2.5}/PM_{10}$ values. Similar to Groups 1-4, Group 5 includes elements that are directly emitted in the particle phase (elements mainly present in primary components), but differs by also including elements for which the major fraction is likely emitted as gases and converted via atmospheric processing to lower volatility products which partition to the particle phase (elements mainly present in secondary components) (Seinfeld and Pandis, 2006). Primary component elements include As, Zn, Se, and Pb (Liu et al., 2017) at all three sites, Sn at Delhi and Krakow, and Cu

255 in Delhi, while secondary component elements comprise Cl, Br, and S (Zhang et al., 2013) at all three sites. Although Cl and Br can in principle relate to primary emission of sea or road-salt, this is unlikely for the sites studied (except London) due to the large distance from the sea, strong and regular diurnal patterns inversely related to temperature, and correlation with elements characteristic of coal combustion and industrial emissions. In London, a major fraction of Cl was attributed to sea/road-salt (Visser et al., 2015a). Further, Xact S and Cl measurements show a strong correlation with AMS-derived non-

260 refractory SO_4^{2-} and Cl^-, respectively, which is nearly insensitive to Cl from sea/road-salt Cl (see Section 2.2). The $PM_{2.5}/PM_{10}$ of these elements is among the highest recorded, with the partial exception of Cl, which is probably due to fact that secondary aerosol condensation is driven by surface area rather than volume. In Delhi, Cl $PM_{2.5}/PM_{10}$ values are high, consistent with a high fraction of NH_4Cl. However, the interquartile range of Cl $PM_{2.5}/PM_{10}$ at Beijing and Krakow is quite wide (0.5 to 0.9), with the lower values approximately matching those of Zn and Pb and suggesting that primary emissions of $ZnCl_2$ and $PbCl_2$

265 are not negligible at these sites.

The primary component elements of Group 5 are strongly linked to various industries and combustion of non-wood fuels. Pb was found to be present in very high concentrations in Delhi with episodic peaks, and possible sources include industrial emissions (Sahu et al., 2011), waste incineration (Kumar et al., 2018), and small-scale Pb-battery recycling units (Jaiprakash et al., 2017). Additionally, burning of plastic and electronic waste can contribute to Pb in Delhi. Zn and As are emitted from a

270 variety of sources, including industries, refuse burning/incineration, and coal combustion, but Zn is also emitted from traffic and wood burning. In Beijing and Krakow, coal burning from coal power plants (Samek, 2012; Yu, 2013) and domestic heating, iron and steel industries (Samek et al., 2018; Yang et al., 2013) are major sources for Zn, Se, As, and Pb. Cu and Sn also have industrial sources, as discussed in connection with Group 4.

The set of potential sources discussed above for the primary Group 5 elements is complex and highly site-dependent, which

275 corresponds to the significant differences between sites evident in the Group 5 correlation matrices (Fig. S10). In Beijing, Pb, Zn, Cl, Br, Se, and S are all tightly correlated, consistent with coal burning emissions. Similar correlations are observed in Krakow, with the exception of Zn and Pb, which are rather correlated with each other, as well as Mn and Fe. The Zn and Pb time series in Krakow contain high intensity plumes (Fig. S12) with a strong peak at ~11:00 LT in $PM_{2.5}$ (Figs. 4 and 5), suggesting industrial emissions (Logiewa et al., 2020). The correlation pattern in Delhi is more complex than at the other sites,

280 with several pairs of tightly correlated elements (e.g., Br and Cl; Se and S) but few larger groupings. This suggests plumes from a variety of point sources rather than a regionally homogeneous composition.

The location-specific influences on primary component elements in Group 5 are also evident in the diurnal patterns. For example, as shown in Fig. 4, the diurnal pattern of Pb is relatively flat in Beijing with a slight rise in the evening, peaks at approximately 08:00-10:00 LT in London, peaks at ~11:00 LT with a tail extending into the afternoon in Krakow, and has a

285 strong diurnal cycle with a massive pre-dawn peak in Delhi. Site-to-site differences are also evident in the location of the elements within the Group 5 box in Fig. 2 (and Fig. S5). Systematic shifts are evident between Beijing (elements clustered to the lower left), Delhi (elements clustered to the upper right; note that two of the elements at the lower left are Cu and Zn, which require a significant shift towards the upper right to even be included in Group 5), and Krakow (intermediate). It is important to note that the y-axes in Figs. 2 and S5 have a logarithmic scale, while the x-axes have a linear scale, which indicates

290 that the graphical vertical shifts represent higher differences than the same graphical horizontal shifts. The mean (± standard deviation) PM_{10el} EFs for Group 5 elements in Delhi, Beijing and Krakow are 1190 (± 1017), 384 (± 357) and 1021 (± 1425), respectively. This site-dependent shift contrasts with Groups 1-3, where no systematic changes are evident. Interestingly, this

appears to be a feature of industrial emissions rather than anthropogenic emissions more generally, as it is not evident in the traffic or biomass combustion-dominated groups (Groups 2 and 3).

4 Discussion and conclusions

The broad intercontinental comparison presented here demonstrates both the large degree of similarity and crucial local differences in the PM_{el} concentration and composition in European and Asian cities. The combination of PM_{10el} EF and $PM_{2.5}/PM_{10}$ provides a robust and useful framework for categorizing elements and assessing site-to-site differences. Five groups are identified based on these metrics (see Fig. 2), with Groups 1-3 having low EF with increasing $PM_{2.5}/PM_{10}$ and Groups 4-5 having high EF with increasing $PM_{2.5}/PM_{10}$. Broadly, Group 1 is related to crustal materials and road dust, Group 2 to non-exhaust traffic emissions, Group 3 to biomass combustion, Group 4 to mixed industrial/traffic emissions, and Group 5 to industrial emissions and coal/waste burning. On an element-by-element basis, the group composition remains relatively consistent across sites, although some reassignment of elements occurs depending on local sources and conditions. Interestingly, we observe systematic shifts within the EF vs. $PM_{2.5}/PM_{10}$ space only for Group 5 (and perhaps in the sparsely populated Group 4), but not in Groups 2 or 3 despite of these groups also being dominated by anthropogenic sources.

However, the consistent classification of elements into a particular group regardless of site does not imply that the temporal behavior of these elements is independent of local conditions or policies. For example, the stagnant meteorological conditions frequently encountered in Beijing during the colder season suppress diurnal variation regardless of element source, while the multitude of strongly emitting point sources yielding individual plumes in Delhi, coupled with rapid dilution as the boundary layer rises, leads to systematic, intense pre-sunrise peaks in concentration but with a composition that strongly varies on a day-to-day basis. The effects of air quality policy are also evident, as the night to day concentration ratios of resuspension-related elements (crustal material, road dust, and non-exhaust traffic emissions) are significantly higher in Delhi and Beijing than in Krakow and London, due to time restrictions on heavy-duty truck activity in the Asian cities.

The diurnal patterns of the total PM_{10el} concentrations (Fig. 4) reflect many of the trends discussed above. Meteorological conditions yield a relatively flat diurnal pattern for Beijing, while concentrations are highest overnight and in the early morning (before rush-hour) in Delhi due to the combined effects of industrial emissions, burning of various solid fuels, and a shallow boundary layer. Krakow and London instead have their highest PM_{10el} concentrations during the day, but features related to the rush-hour are more visible in Krakow, whereas the London diurnals are similar to that of resuspended dust (Visser et al., 2015a). This may reflect differences in the fleet composition, specifically a higher fraction of older vehicles, vehicles with faulty catalytic converters or diesel particulate filters in Krakow (Majewski et al., 2018).

The global similarities and local differences discussed above should be considered in air quality policy formulation. Current practices focus mainly on total PM mass reduction, neglecting its toxicity. As an example, the carcinogenic elements represent a specific health concern. These elements are not assigned to a single group by the EF vs. $PM_{2.5}/PM_{10}$, and the group(s) to which they are assigned do not necessarily correlate with total PM_{10el}. While such policies may have significant ancillary benefits, they may not efficiently address the most critical health risks. In addition, the inhalability of potential toxins needs consideration; Pb and As (which are more industry-related) have $PM_{2.5}/PM_{10}$ values that are up to 3 times higher than those of Ni and Cr (which are more traffic-related). If size dependence is not considered, inefficient or ineffective regulatory priorities may result. Finally, this study demonstrates that regulatory policy can affect not only overall concentrations but also the timing of daily maxima (e.g., truck activity restrictions in Delhi and Beijing). The above considerations highlight the importance of time- and size-resolved measurements for policy formulation, as well as the need to integrate these with daily human activities. Although the method proposed in this work allows for a comparison of the characteristics in different cities, a full SA analysis is necessary if more quantitative information (e.g., source contributions) is desired.

Data availability

The data presented in the text and figures as well as in the supplement will be available upon publication of the final manuscript
335 (https://zenodo.org). Additional related data can be made available by the corresponding authors (MF and ASHP) upon request.

Author contributions

PR and JGS wrote the paper with input from all co-authors. PR, MF, DB, YT, VK, AKT, LW, SV, AS, and JN designed the study. GW designed ISS in Xact. YT and AP analyzed AMS data. PR analyzed Xact data. SV, MF, and JGS provided offline data for London. ASHP, JGS, MF, IEH, and UB were involved with the supervision. ASHP, JGS, MF and UB assisted in the
340 interpretation of the results.

Competing interests

The authors declare no competing financial interests.

References

Amato, F., Pandolfi, M., Escrig, A., Querol, X., Alastuey, A., Pey, J., Perez, N., and Hopke, P. K.: Quantifying road dust
355 resuspension in urban environment by Multilinear Engine: A comparison with PMF2, Atmos. Environ., 43, 2770–2780, https://doi.org/10.1016/j.atmosenv.2009.02.039, 2009.

An, Z., Huang, R. J., Zhang, R., Tie, X., Li, G., Cao, J., Zhou, W., Shi, Z., Han, Y., Gu, Z., and Ji, Y.: Severe haze in northern China: A synergy of anthropogenic emissions and atmospheric processes, Proc. Natl. Acad. Sci. USA, 116, 8657–8666, https://doi.org/10.1073/pnas.1900125116, 2019.

360 Bigi, A. and Harrison, R. M.: Analysis of the air pollution climate at a central urban background site, Atmos. Environ., 44, 2004–2012, https://doi.org/10.1016/j.atmosenv.2010.02.028, 2010.

Bukowiecki, N., Lienemann, P., Zwicky, C. N., Furger, M., Richard, A., Falkenberg, G., Rickers, K., Grolimund, D., Borca, C., Hill, M., Gehrig, R., and Baltensperger, U.: X-ray fluorescence spectrometry for high throughput analysis of atmospheric aerosol samples: The benefits of synchrotron X-rays, Spectrochim. Acta B, 63, 929–938,
365 https://doi.org/10.1016/j.sab.2008.05.006, 2008.

Bukowiecki, N., Lienemann, P., Hill, M., Furger, M., Richard, A., Amato, F., Prévôt, A. S. H., Baltensperger, U., Buchmann, B., and Gehrig, R.: PM_{10} emission factors for non-exhaust particles generated by road traffic in an urban street canyon and along a freeway in Switzerland, Atmos. Environ., 44, 2330–2340, https://doi.org/10.1016/j.atmosenv.2010.03.039, 2010.

370 Canagaratna, M. R., Jayne, J. T., Jimenez, J. L., Allan, J. D., Alfarra, M. R., Zhang, Q., Onasch, T. B., Drewnick, F., Coe, H., Middlebrook, A., Delia, A., Williams, L. R., Trimborn, A. M., Northway, M. J., DeCarlo, P. F., Kolb, C. E., Davidovits, P., and Worsnop, D. R.: Chemical and microphysical characterization of ambient aerosols with the aerodyne aerosol mass spectrometer, Mass Spectrom. Rev., 26, 185–222, https://doi.org/10.1002/mas.20115, 2007.

Chang, Y., Huang, K., Xie, M., Deng, C., Zou, Z., Liu, S., and Zhang, Y.: First long-term and near real-time measurement of trace elements in China's urban atmosphere: temporal variability, source apportionment and precipitation effect, Atmos. Chem. Phys., 18, 11793–11812, https://doi.org/10.5194/acp-18-11793-2018, 2018.

375 Cheng, Y., Lee, S., Gu, Z., Ho, K., Zhang, Y., Huang, Y., Chow, J. C., Watson, J. G., Cao, J., and Zhang, R.: $PM_{2.5}$ and $PM_{10-2.5}$ chemical composition and source apportionment near a Hong Kong roadway, Partic., 18, 96–104, https://doi.org/10.1016/j.partic.2013.10.003, 2015.

Cooper, J. A., Petterson, K., Geiger, A., and Siemers, A.: Guide for developing a multi-metals, fence-line monitoring plan for 380 fugitive emissions using X-ray based monitors, Cooper Environmental Services, Portland, Oregon, https://www3.epa.gov/ttn/emc/prelim/otm31.pdf, (last access: 28 October, 2020), 2010.

Dall'Osto, M., Querol, X., Amato, F., Karanasiou, A., Lucarelli, F., Nava, S., Calzolai, G., and Chiari, M.: Hourly elemental concentrations in $PM_{2.5}$ aerosols sampled simultaneously at urban background and road site during SAPUSS – diurnal variations and PMF receptor modelling, Atmos. Chem. Phys., 13, 4375–4392, https://doi.org/10.5194/acp-13-4375-2013, 385 2013.

Das, R., Khezri, B., Srivastava, B., Datta, S., Sikdar, P. K., Webster, R. D., and Wang, X.: Trace element composition of $PM_{2.5}$ and PM_{10} from Kolkata – a heavily polluted Indian metropolis, Atmos. Pollut. Res., 6, 742–750, https://doi.org/10.5094/APR.2015.083, 2015.

EEA: Air quality in Europe—2018 report, Copenhagen, 2018, available at: https://www.eea.europa.eu/publications/air-390 quality-in-europe-2018/at_download/file, (last access: 5 June, 2020), 2018.

Flechsig, U., Jaggi, A., Spielmann, S., Padmore, H. A., and MacDowell, A. A.: The optics beamline at the Swiss Light Source, Nucl. Inst. Meth. Phys. Res. Sect. A: Accel., Spect., Detec. Assoc. Equip., 609, 281–285, https://doi.org/10.1016/j.nima.2009.07.092, 2009.

Fomba, K. W., Müller, K., van Pinxteren, D., and Herrmann, H.: Aerosol size-resolved trace metal composition in remote 395 northern tropical Atlantic marine environment: case study Cape Verde islands, Atmos. Chem. Phys., 13, 4801–4814, https://doi.org/10.5194/acp-13-4801-2013, 2013.

Fomba, K. W., Müller, K., van Pinxteren, D., Poulain, L., van Pinxteren, M., and Herrmann, H.: Long-term chemical characterization of tropical and marine aerosols at the Cape Verde Atmospheric Observatory (CVAO) from 2007 to 2011, Atmos. Chem. Phys., 14, 8883–8904, https://doi.org/10.5194/acp-14-8883-2014, 2014.

400 Furger, M., Minguillón, M. C., Yadav, V., Slowik, J. G., Hüglin, C., Fröhlich, R., Petterson, K., Baltensperger, U., and Prévôt, A. S. H.: Elemental composition of ambient aerosols measured with high temporal resolution using an online XRF spectrometer, Atmos. Meas. Tech., 10, 2061–2076, https://doi.org/10.5194/amt-10-2061-2017, 2017.

Furger, M., Rai, P., Slowik, J. G., Cao, J., Visser, S., Baltensperger, U., and Prévôt, A. S. H.: Automated alternating sampling of PM_{10} and $PM_{2.5}$ with an online XRF spectrometer, Atmos. Environ.: X, 5, 100065,
405 https://doi.org/10.1016/j.aeaoa.2020.100065, 2020.

Gao, W., Tang, G., Ji, D., Liu Z., Song, T., Cheng, M., and Wang, Y.: Implementation effects and countermeasures of China′s air pollution prevention and control action plan, Res. Environ. Sci, 29 (11), 1567–1574 https://doi.org/10.13198/j.issn.1001-6929.2016.11.01, 2016 (in Chinese).

Grigoratos, T. and Martini, G.: Brake wear particle emissions: a review, Environ. Sci. Pollut. Res., 22, 2491–2504,
410 https://doi.org/10.1007/s11356-014-3696-8, 2015.

Gupta, I., Salunkhe, A., and Kumar, R.: Source apportionment of PM_{10} by positive matrix factorization in urban area of Mumbai, India, Sci. World J., 2012, 585791, https://doi.org/10.1100/2012/585791, 2012.

Hjortenkrans, D. S. T., Bergback, B. G., and Haggerud, A. V.: Metal emissions from brake linings and tires: Case studies of Stockholm, Sweden 1995/1998 and 2005, Environ. Sci. Technol., 41, 5224–5230, https://doi.org/10.1021/es070198o, 2007.

415 IARC: Agents classified by the IARC monographs, 1–127, available at: https://monographs.iarc.fr/agents-classified-by-the-iarc/, last access: 4 July, 2020.

Iijima, A., Sato, K., Yano, K., Tago, H., Kato, M., Kimura, H., and Furuta, N.: Particle size and composition distribution analysis of automotive brake abrasion dusts for the evaluation of antimony sources of airborne particulate matter, Atmos. Environ., 41, 4908–4919, https://doi.org/10.1016/j.atmosenv.2007.02.005, 2007.

420 Jaiprakash, Singhai, A., Habib, G., Raman, R. S., and Gupta, T.: Chemical characterization of $PM_{1.0}$ aerosol in Delhi and source apportionment using positive matrix factorization, Environ. Sci. Pollut. Res., 24, 445–462, https://doi.org/10.1007/s11356-016-7708-8, 2017.

Jaishankar, M., Tseten, T., Anbalagan, N., Mathew, B. B., and Beeregowda, K. N.: Toxicity, mechanism and health effects of some heavy metals, Interdis. toxicol., 7 (2), 60–72, https://doi.org/10.2478/intox-2014-0009, 2014.

425 Junninen, H., Monster, J., Rey, M., Cancelinha, J., Douglas, K., Duane, M., Forcina, V., Mueller, A., Lagler, F., Marelli, L., Borowiak, A., Niedzialek, J., Paradiz, B., Mira-Salama, D., Jimenez, J., Hansen, U., Astorga, C., Stanczyk, K., Viana, M., Querol, X., Duvall, R. M., Norris, G. A., Tsakovski, S., Wahlin, P., Horak, J., and Larsen, B. R.: Quantifying the impact of residential heating on the urban air quality in a typical European coal combustion region, Environ. Sci. Technol., 43, 7964–7970, https://doi.org/10.1021/es8032082, 2009.

430 Kelly, F. J. and Fussell, J. C.: Size, source and chemical composition as determinants of toxicity attributable to ambient particulate matter, Atmos. Environ., 60, 504–526, https://doi.org/10.1016/j.atmosenv.2012.06.039, 2012.

Krzyzanowski, M., Apte, J. S., Bonjour, S. P., Brauer, M., Cohen, A. J., and Prüss-Ustun, A. M.: Air pollution in the megacities, Current Environ. Health Rep., 1, 185–191, https://doi.org/10.1007/s40572-014-0019-7, 2014.

Kumar, P., Gulia, S., Harrison, R. M., and Khare, M.: The influence of odd-even car trial on fine and coarse particles in Delhi, Environ. Pollut., 225, 20–30, https://doi.org/10.1016/j.envpol.2017.03.017, 2017.

Kumar, S., Aggarwal, S. G., Gupta, P. K., and Kawamura, K.: Investigation of the tracers for plastic-enriched waste burning aerosols, Atmos. Environ., 108, 49–58, https://doi.org/10.1016/j.atmosenv.2015.02.066, 2015.

Kumar, S., Aggarwal, S. G., Sarangi, B., Malherbe, J., Barre, J. P. G., Berail, S., Séby, F., and Donard, O. F. X.: Understanding the influence of open-waste burning on urban aerosols using metal tracers and lead isotopic composition, Aerosol Air Qual. Res., 18, 2433–2446, https://doi.org/10.4209/aaqr.2017.11.0510, 2018.

Lim, S. S., Vos, T., Flaxman, A. D., Danaei, G., Shibuya, K., Adair-Rohani, H., AlMazroa, M. A., Amann, M., Anderson, H. R., Andrews, K. G., Aryee, M., Atkinson, C., Bacchus, L. J., Bahalim, A. N., Balakrishnan, K., Balmes, J., Barker-Collo, S., Baxter, A., Bell, M. L., Blore, J. D., Blyth, F., Bonner, C., Borges, G., Bourne, R., Boussinesq, M., Brauer, M., Brooks, P., Bruce, N. G., Brunekreef, B., Bryan-Hancock, C., Bucello, C., Buchbinder, R., Bull, F., Burnett, R. T., Byers, T. E., Calabria, B., Carapetis, J., Carnahan, E., Chafe, Z., Charlson, F., Chen, H., Chen, J. S., Cheng, A. T.-A., Child, J. C., Cohen, A., Colson, K. E., Cowie, B. C., Darby, S., Darling, S., Davis, A., Degenhardt, L., Dentener, F., Des Jarlais, D. C., Devries, K., Dherani, M., Ding, E. L., Dorsey, E. R., Driscoll, T., Edmond, K., Ali, S. E., Engell, R. E., Erwin, P. J., Fahimi, S., Falder, G., Farzadfar, F., Ferrari, A., Finucane, M. M., Flaxman, S., Fowkes, F. G. R., Freedman, G., Freeman, M. K., Gakidou, E., Ghosh, S., Giovannucci, E., Gmel, G., Graham, K., Grainger, R., Grant, B., Gunnell, D., Gutierrez, H. R., Hall, W., Hoek, H. W., Hogan, A., Hosgood, H. D., Hoy, D., Hu, H., Hubbell, B. J., Hutchings, S. J., Ibeanusi, S. E., Jacklyn, G. L., Jasrasaria, R., Jonas, J. B., Kan, H., Kanis, J. A., Kassebaum, N., Kawakami, N., Khang, Y.-H., Khatibzadeh, S., Khoo, J.-P., Kok, C., Laden, F., Lalloo, R., Lan, Q., Lathlean, T., Leasher, J. L., Leigh, J., Li, Y., Lin, J. K., Lipshultz, S. E., London, S., Lozano, R., Lu, Y., Mak, J., Malekzadeh, R., Mallinger, L., Marcenes, W., March, L., Marks, R., Martin, R., McGale, P., McGrath, J., Mehta, S., Memish, Z. A., Mensah, G. A., Merriman, T. R., Micha, R., Michaud, C., Mishra, V., Hanafiah, K. M., Mokdad, A. A., Morawska, L., Mozaffarian, D., Murphy, T., Naghavi, M., Neal, B., Nelson, P. K., Nolla, J. M., Norman, R., Olives, C., Omer, S. B., Orchard, J., Osborne, R., Ostro, B., Page, A., Pandey, K. D., Parry, C. D. H., Passmore, E., Patra, J., Pearce, N., Pelizzari, P. M., Petzold, M., Phillips, M. R., Pope, D., Pope, C. A., Powles, J., Rao, M., Razavi, H., Rehfuess, E. A., Rehm, J. T., Ritz, B., Rivara, F. P., Roberts, T., Robinson, C., Rodriguez-Portales, J. A., Romieu, I., Room, R., Rosenfeld, L. C., Roy, A., Rushton, L., Salomon, J. A., Sampson, U., Sanchez-Riera, L., Sanman, E., Sapkota, A., Seedat, S., Shi, P., Shield, K., Shivakoti, R., Singh, G. M., Sleet, D. A., Smith, E., Smith, K. R., Stapelberg, N. J. C., Steenland, K., Stöckl, H., Stovner, L. J., Straif, K., Straney, L., Thurston, G. D., Tran, J. H., Van Dingenen, R., van Donkelaar, A., Veerman, J. L., Vijayakumar, L., Weintraub, R., Weissman, M. M., White, R. A., Whiteford, H., Wiersma, S. T., Wilkinson, J. D., Williams, H. C., Williams, W., Wilson, N., Woolf, A. D., Yip, P., Zielinski, J. M., Lopez, A. D., Murray, C. J. L., and Ezzati, M.: A comparative risk assessment of burden of disease and injury attributable to 67 risk factors and risk factor clusters in 21 regions, 1990–2010: a systematic analysis for the Global Burden of Disease Study 2010, The Lancet, 380, 2224–2260, https://doi.org/10.1016/s0140-6736(12)61766-8, 2012.

Liu, L., Kong, S., Zhang, Y., Wang, Y., Xu, L., Yan, Q., Lingaswamy, A. P., Shi, Z., Lv, S., Niu, H., Shao, L., Hu, M., Zhang, D., Chen, J., Zhang, X., and Li, W.: Morphology, composition, and mixing state of primary particles from combustion sources—crop residue, wood, and solid waste, Sci. Rep., 7, 1–15, https://doi.org/10.1038/s41598-017-05357-2, 2017.

Logiewa, A., Miazgowicz, A., Krennhuber, K., and Lanzerstorfer, C.: Variation in the concentration of metals in road dust size fractions between 2 µm and 2 mm: results from three metallurgical centres in Poland, Arch. Environ. Contam. Toxicol., 78, 46–59, https://doi.org/10.1007/s00244-019-00686-x, 2020.

Maenhaut, W., Raes, N., and Wang, W.: Analysis of atmospheric aerosols by particle induced X-ray emission, instrumental neutron activation analysis, and ion chromatography, Nucl. Inst. Meth. Phys. Res. Sect. B: Beam Interact. Mater. Atoms., 269, 2693–2698, https://doi.org/10.1016/j.nimb.2011.08.012, 2011.

Majewski, G. and Rogula-Kozłowska, W.: The elemental composition and origin of fine ambient particles in the largest Polish conurbation: first results from the short-term winter campaign, Theor. Appl. Climat., 125, 79–92, https://doi.org/10.1007/s00704-015-1494-y, 2016.

Majewski, G., Rogula-Kozłowska, W., Rozbicka, K., Rogula-Kopiec, P., Mathews, B., and Brandyk, A.: Concentration, chemical composition and origin of PM_1: results from the first long-term measurement campaign in Warsaw (Poland), Aerosol Air Qual. Res., 18, 636–654, https://doi.org/10.4209/aaqr.2017.06.0221, 2018.

Manke, A., Wang, L., and Rojanasakul, Y.: Mechanisms of nanoparticle-induced oxidative stress and toxicity, Biomed. Res. Int., 2013, 942916, https://doi.org/10.1155/2013/942916, 2013.

Miller, F. J., Gardner, D. E., Graham, J. A., Lee, R. E., Wilson, W. E., and Bachmann, J. D.: Size considerations for establishing a standard for inhalable particles, J. Air Pollut. Control Assoc., 29, 610–615, https://doi.org/10.1080/00022470.1979.10470831, 1979.

Moreno, T., Karanasiou, A., Amato, F., Lucarelli, F., Nava, S., Calzolai, G., Chiari, M., Coz, E., Artíñano, B., Lumbreras, J., Borge, R., Boldo, E., Linares, C., Alastuey, A., Querol, X., and Gibbons, W.: Daily and hourly sourcing of metallic and mineral dust in urban air contaminated by traffic and coal-burning emissions, Atmos. Environ., 68, 33–44, https://doi.org/10.1016/j.atmosenv.2012.11.037, 2013.

Owoade, K. O., Hopke, P. K., Olise, F. S., Ogundele, L. T., Fawole, O. G., Olaniyi, B. H., Jegede, O. O., Ayoola, M. A., and Bashiru, M. I.: Chemical compositions and source identification of particulate matter ($PM_{2.5}$ and $PM_{2.5–10}$) from a scrap iron and steel smelting industry along the Ife–Ibadan highway, Nigeria. Atmos. Pollut. Res., 6 (1), 107–119, https://doi.org/10.5094/APR.2015.013, 2015.

Pant, P. and Harrison, R. M.: Critical review of receptor modelling for particulate matter: a case study of India, Atmos. Environ., 49, 1–12, https://doi.org/10.1016/j.atmosenv.2011.11.060, 2012.

Pant, P., Baker, S. J., Shukla, A., Maikawa, C., Godri Pollitt, K. J., and Harrison, R. M.: The PM_{10} fraction of road dust in the UK and India: Characterization, source profiles and oxidative potential, Sci. Total Environ., 530–531, 445–452, https://doi.org/10.1016/j.scitotenv.2015.05.084, 2015.

Rahman, S. A., Hamzah, M. S., Wood, A. K., Elias, M. S., Salim, N. A. A., and Sanuri, E.: Sources apportionment of fine and coarse aerosol in Klang Valley, Kuala Lumpur using positive matrix factorization, Atmos. Pollut. Res., 2, 197–206, https://doi.org/10.5094/APR.2011.025, 2011.

Rahn, K. A.: Silicon and aluminum in atmospheric aerosols: crust air fractionation?, Atmos. Environ., 10, 597–601, https://doi.org/10.1016/0004-6981(76)90044-5, 1976.

Rai, P., Furger, M., El Haddad, I., Kumar, V., Wang, L., Singh, A., Dixit, K., Bhattu, D., Petit, J.-E., Ganguly, D., Rastogi, N., Baltensperger, U., Tripathi, S. N., Slowik, J. G., and Prévôt, A. S. H.: Real-time measurement and source apportionment of elements in Delhi's atmosphere, Sci. Total Environ., 742, 140332, https://doi.org/10.1016/j.scitotenv.2020.140332, 2020.

Richard, A., Bukowiecki, N., Lienemann, P., Furger, M., Fierz, M., Minguillón, M. C., Weideli, B., Figi, R., Flechsig, U., Appel, K., Prévôt, A. S. H., and Baltensperger, U.: Quantitative sampling and analysis of trace elements in atmospheric aerosols: impactor characterization and Synchrotron-XRF mass calibration, Atmos. Meas. Tech., 3, 1473–1485, https://doi.org/10.5194/amt-3-1473-2010, 2010.

Rogula-Kozłowska, W.: Size-segregated urban particulate matter: mass closure, chemical composition, and primary and secondary matter content, Air Qual. Atmos. Health, 9, 533–550, https://doi.org/10.1007/s11869-015-0359-y, 2016.

Rogula-Kozłowska, W., Klejnowski, K., Rogula-Kopiec, P., Mathews, B., and Szopa, S.: A study on the seasonal mass closure of ambient fine and coarse dusts in Zabrze, Poland, Bullet. Environ. Contam. Toxicol., 88, 722–729, https://doi.org/10.1007/s00128-012-0533-y, 2012.

Rudnik, R. and Gao, S.: Composition of the continental crust, in: The Crust, Vol. 3, edited by: Rudnick, E., Book Sect. 2, 1–56, Elsevier Sci. Philadelphia, 2003.

Sahu, M., Hu, S., Ryan, P. H., Le Masters, G., Grinshpun, S. A., Chow, J. C., and Biswas, P.: Chemical compositions and source identification of $PM_{2.5}$ aerosols for estimation of a diesel source surrogate, Sci. Total Environ., 409, 2642–2651, https://doi.org/10.1016/j.scitotenv.2011.03.032, 2011.

Samek, L.: Source apportionment of the PM_{10} fraction of particulate matter collected in Kraków, Poland, Nukleo., 57 (4), 601–606, 2012.

Samek, L., Stegowski, Z., Furman, L., and Fiedor, J.: Chemical content and estimated sources of fine fraction of particulate matter collected in Krakow, Air Qual. Atmos. Health, 10, 47–52, https://doi.org/10.1007/s11869-016-0407-2, 2017a.

Samek, L., Stegowski, Z., Furman, L., Styszko, K., Szramowiat, K., and Fiedor, J.: Quantitative assessment of $PM_{2.5}$ sources and their seasonal variation in Krakow, Water Air Soil Pollut., 228, 290, https://doi.org/10.1007/s11270-017-3483-5, 2017b.

Samek, L., Stegowski, Z., Styszko, K., Furman, L., and Fiedor, J.: Seasonal contribution of assessed sources to submicron and fine particulate matter in a Central European urban area, Environ. Pollut., 241, 406–411, https://doi.org/10.1016/j.envpol.2018.05.082, 2018.

Shah, S.: Poland finally realizes it has to deal with its pollution problem-Emerging Europe, News, Intelligence, Community, available at: https://emerging-europe.com/news/poland-finally-realises-it-has-to-deal-with-its-pollution-problem, (last access: 28 October, 2020), 2018.

Seinfeld, J. H. and Pandis, S. N.: Atmospheric chemistry and physics: from air pollution to climate change, Eds. 2, John Wiley & Sons, Inc., New York, USA, 2006.

Srimuruganandam, B. and Nagendra, S. M. S.: Source characterization of PM_{10} and $PM_{2.5}$ mass using a chemical mass balance model at urban roadside, Sci. Total Environ., 433, 8–19, https://doi.org/10.1016/j.scitotenv.2012.05.082, 2012.

Tao, J., Zhang, L., Engling, G., Zhang, R., Yang, Y., Cao, J., Zhu, C., Wang, Q., and Luo, L.: Chemical composition of $PM_{2.5}$ in an urban environment in Chengdu, China: Importance of springtime dust storms and biomass burning, Atmos. Res., 122, 270–283, https://doi.org/10.1016/j.atmosres.2012.11.004, 2013.

14

Tauler, R., Viana, M., Querol, X., Alastuey, A., Flight, R. M., Wentzell, P. D., and Hopke, P. K.: Comparison of the results obtained by four receptor modelling methods in aerosol source apportionment studies, Atmos. Environ., 43, 3989–3997, https://doi.org/10.1016/j.atmosenv.2009.05.018, 2009.

Thorpe, A. and Harrison, R. M.: Sources and properties of non-exhaust particulate matter from road traffic: a review, Sci. Total Environ., 400, 270–282, https://doi.org/10.1016/j.scitotenv.2008.06.007, 2008.

Tian, H. Z., Zhu, C. Y., Gao, J. J., Cheng, K., Hao, J. M., Wang, K., Hua, S. B., Wang, Y., and Zhou, J. R.: Quantitative assessment of atmospheric emissions of toxic heavy metals from anthropogenic sources in China: historical trend, spatial distribution, uncertainties, and control policies, Atmos. Chem. Phys., 15, 10127–10147, https://doi.org/10.5194/acp-15-10127-2015, 2015.

Tremper, A. H., Font, A., Priestman, M., Hamad, S. H., Chung, T.-C., Pribadi, A., Brown, R. J. C., Goddard, S. L., Grassineau, N., Petterson, K., Kelly, F. J., and Green, D. C.: Field and laboratory evaluation of a high time resolution x-ray fluorescence instrument for determining the elemental composition of ambient aerosols, Atmos. Meas. Tech., 11, 3541–3557, https://doi.org/10.5194/amt-11-3541-2018, 2018.

USEPA: Regional Screening Levels (RSLs), available at: www.epa.gov/risk/regional-screening-levels-rsls-generic-tables, last access: 20 June, 2020.

Venter, A. D., van Zyl, P. G., Beukes, J. P., Josipovic, M., Hendriks, J., Vakkari, V., and Laakso, L.: Atmospheric trace metals measured at a regional background site (Welgegund) in South Africa, Atmos. Chem. Phys., 17, 4251–4263, https://doi.org/10.5194/acp-17-4251-2017, 2017.

Viana, M., Kuhlbusch, T. A. J., Querol, X., Alastuey, A., Harrison, R. M., Hopke, P. K., Winiwarter, W., Vallius, M., Szidat, S., Prévôt, A. S. H., Hueglin, C., Bloemen, H., Wåhlin, P., Vecchi, R., Miranda, A. I., Kasper-Giebl, A., Maenhaut, W., and Hitzenberger, R.: Source apportionment of particulate matter in Europe: a review of methods and results, J. Aerosol Sci., 39, 827–849, https://doi.org/10.1016/j.jaerosci.2008.05.007, 2008.

Viana, M., Reche, C., Amato, F., Alastuey, A., Querol, X., Moreno, T., Lucarelli, F., Nava, S., Calzolai, G., Chiari, M., and Rico, M.: Evidence of biomass burning aerosols in the Barcelona urban environment during winter time, Atmos. Environ., 72, 81–88, https://doi.org/10.1016/j.atmosenv.2013.02.031, 2013.

Vincent, K. and Passant, N.: Assessment of heavy metal concentrations in the United Kingdom. Report to the Department for Environment, Food and Rural Affairs, Welsh Assembly Government, the Scottish Executive and the Department of the Environment for Northern Ireland. AEAT/ENV/R/2013/Issue 1, AEA Technology, https://uk-air.defra.gov.uk/assets/documents/reports/cat16/0604041205_heavy_metal_issue1_final.pdf, (last access: 28 October, 2020), 2006.

Visser, S., Slowik, J. G., Furger, M., Zotter, P., Bukowiecki, N., Canonaco, F., Flechsig, U., Appel, K., Green, D. C., Tremper, A. H., Young, D. E., Williams, P. I., Allan, J. D., Coe, H., Williams, L. R., Mohr, C., Xu, L., Ng, N. L., Nemitz, E., Barlow, J. F., Halios, C. H., Fleming, Z. L., Baltensperger, U., and Prévôt, A. S. H.: Advanced source apportionment of size-resolved trace elements at multiple sites in London during winter, Atmos. Chem. Phys., 15, 11291–11309, https://doi.org/10.5194/acp-15-11291-2015, 2015a.

Visser, S., Slowik, J. G., Furger, M., Zotter, P., Bukowiecki, N., Dressler, R., Flechsig, U., Appel, K., Green, D. C., Tremper, A. H., Young, D. E., Williams, P. I., Allan, J. D., Herndon, S. C., Williams, L. R., Mohr, C., Xu, L., Ng, N. L., Detournay, A., Barlow, J. F., Halios, C. H., Fleming, Z. L., Baltensperger, U., and Prévôt, A. S. H.: Kerb and urban increment of highly time-resolved trace elements in PM_{10}, $PM_{2.5}$ and $PM_{1.0}$ winter aerosol in London during ClearfLo 2012, Atmos. Chem. Phys., 15,
580   2367–2386, https://doi.org/10.5194/acp-15-2367-2015, 2015b.

Waked, A., Favez, O., Alleman, L. Y., Piot, C., Petit, J.-E., Delaunay, T., Verlinden, E., Golly, B., Besombes, J. L., Jaffrezo, J. L., and Leoz-Garziandia, E.: Source apportionment of PM_{10} in a north-western Europe regional urban background site (Lens, France) using positive matrix factorization and including primary biogenic emissions, Atmos. Chem. Phys., 14, 3325–3346, https://doi.org/10.5194/acp-14-3325-2014, 2014.

585   Wei, F., Teng, E., Wu, G., Hu, W., Wilson, W. E., Chapman, R. S., Pau, J. C., and Zhang, J.: Ambient concentrations and elemental compositions of PM_{10} and $PM_{2.5}$ in four Chinese cities, Environ. Sci. Technol., 33, 4188–4193, https://doi.org/10.1021/es9904944, 1999.

Yang, L., Cheng, S., Wang, X., Nie, W., Xu, P., Gao, X., Yuan, C., and Wang, W.: Source identification and health impact of $PM_{2.5}$ in a heavily polluted urban atmosphere in China, Atmos. Environ., 75, 265–269,
590   https://doi.org/10.1016/j.atmosenv.2013.04.058, 2013.

Yao, X. H., Chan, C. K., Fang, M., Cadle, S., Chan, T., Mulawa, P., He, K. B., and Ye, B. M.: The water-soluble ionic composition of $PM_{2.5}$ in Shanghai and Beijing, China, Atmos. Environ., 36, 4223–4234, https://doi.org/10.1016/S1352-2310(02)00342-4, 2002.

Yu, L.: Characterization and source apportionment of $PM_{2.5}$ in an urban environment in Beijing, Aerosol Air Qual. Res., 13,
595   574–583, https://doi.org/10.4209/aaqr.2012.07.0192, 2013.

Zhang, B., Zhou, T., Liu, Y., Yan, C., Li, X., Yu, J., Wang, S., Liu, B., and Zheng, M.: Comparison of water-soluble inorganic ions and trace metals in $PM_{2.5}$ between online and offline measurements in Beijing during winter, Atmos. Pollut. Res., 10, 1755-1765, 10.1016/j.apr.2019.07.007, 2019.

Zhang, R., Jing, J., Tao, J., Hsu, S.-C., Wang, G., Cao, J., Lee, C. S. L., Zhu, L., Chen, Z., Zhao, Y., and Shen, Z.: Chemical
600   characterization and source apportionment of $PM_{2.5}$ in Beijing: seasonal perspective, Atmos. Chem. Phys., 13, 7053–7074, https://doi.org/10.5194/acp-13-7053-2013, 2013.

Zhao, R., Han, B., Lu, B., Zhang, N., Zhu, L., and Bai, Z.: Element composition and source apportionment of atmospheric aerosols over the China Sea, Atmos. Pollut. Res., 6, 191–201, https://doi.org/10.5094/APR.2015.023, 2015.

Zheng, G. J., Duan, F. K., Su, H., Ma, Y. L., Cheng, Y., Zheng, B., Zhang, Q., Huang, T., Kimoto, T., Chang, D., Pöschl, U.,
605   Cheng, Y. F., and He, K. B.: Exploring the severe winter haze in Beijing: the impact of synoptic weather, regional transport and heterogeneous reactions, Atmos. Chem. Phys., 15, 2969–2983, https://doi.org/10.5194/acp-15-2969-2015, 2015.
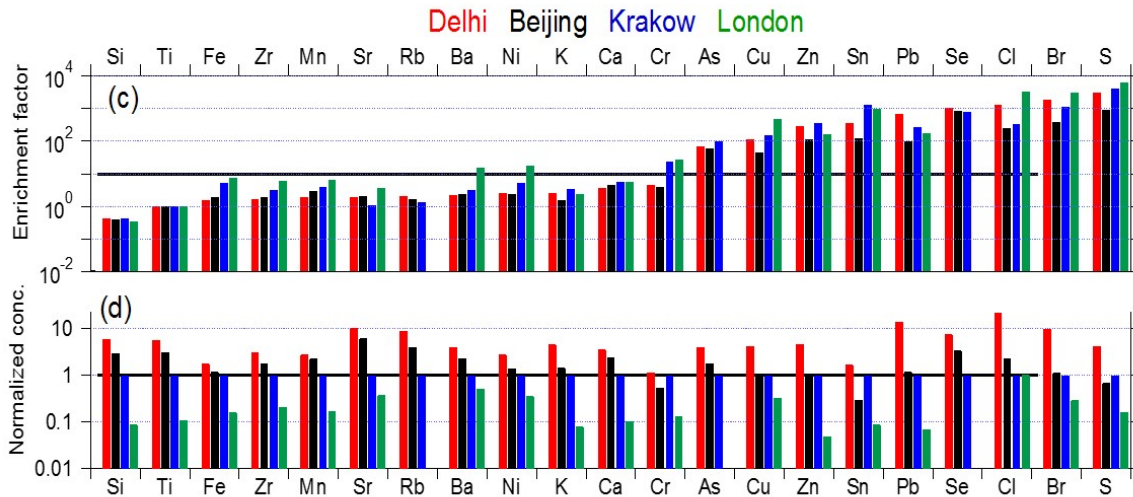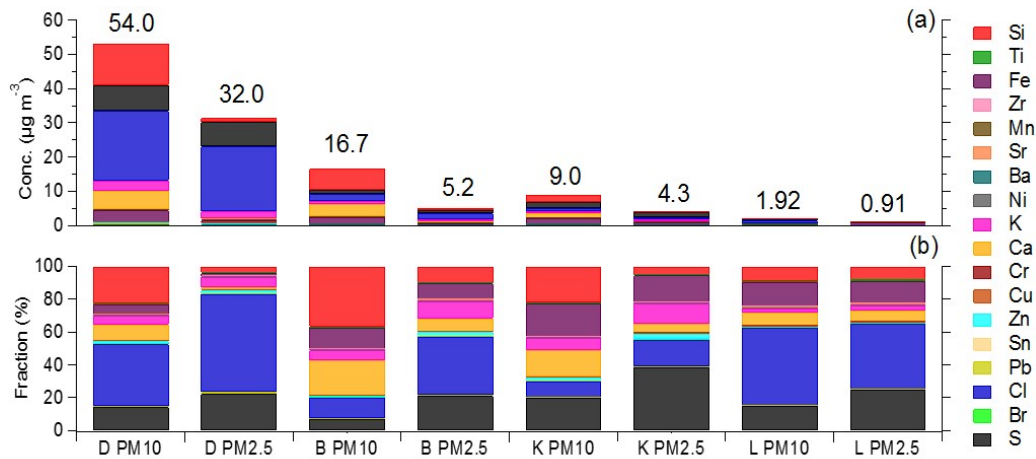
Figure 1: (a) Averaged elemental concentrations and **(b)** fractions (%) of elements in both size ranges at all four sites (Delhi (D), Beijing (B), Krakow (K), London (L)); **(c)** Enrichment factors (using Ti as reference) of the measured elements in PM$_{10}$ (EF ~10 (solid line)); **(d)** averaged elemental concentrations in PM$_{10}$ normalized by those at Krakow. Note that Rb, As and Se are not included in (a) and (b) because of absence in the London dataset, while all three are considered in (c) and (d) for the comparison between the rest of the sites.
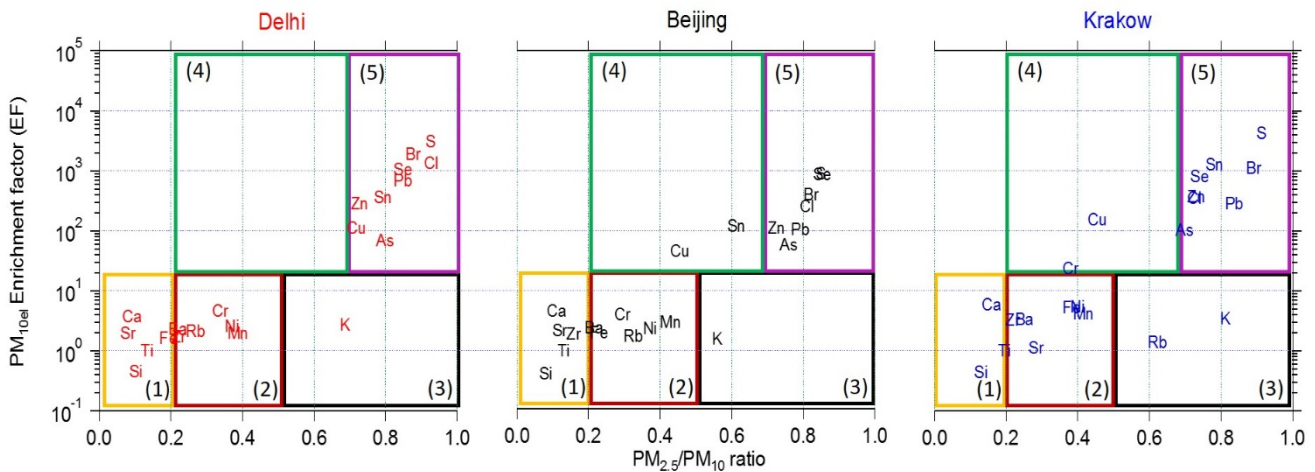

Figure 2: Classification of the measured elements in five groups for Delhi, Beijing, and Krakow based on their PM$_{10}$ enrichment factor (EF) vs PM$_{2.5}$/PM$_{10}$ values. PM$_{10}$ EF vs PM$_{2.5}$/PM$_{10}$ values and PM$_{2.5}$ EF vs PM$_{2.5}$/PM$_{10}$ values for all four sites are shown in Supplementary (Fig. S5).

17
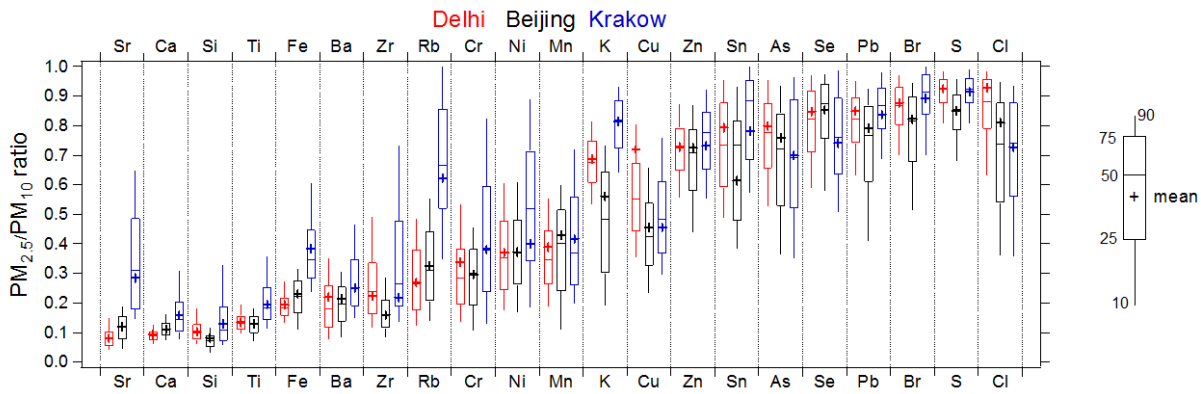
Figure 3: Box-whisker plots of the measured elemental PM$_{2.5}$/PM$_{10}$ ratios at Delhi, Beijing, and Krakow (see Fig. S4 for all four sites). Box: First to third quartile range, −: median line, +: mean, whiskers: 10-90% percentiles.
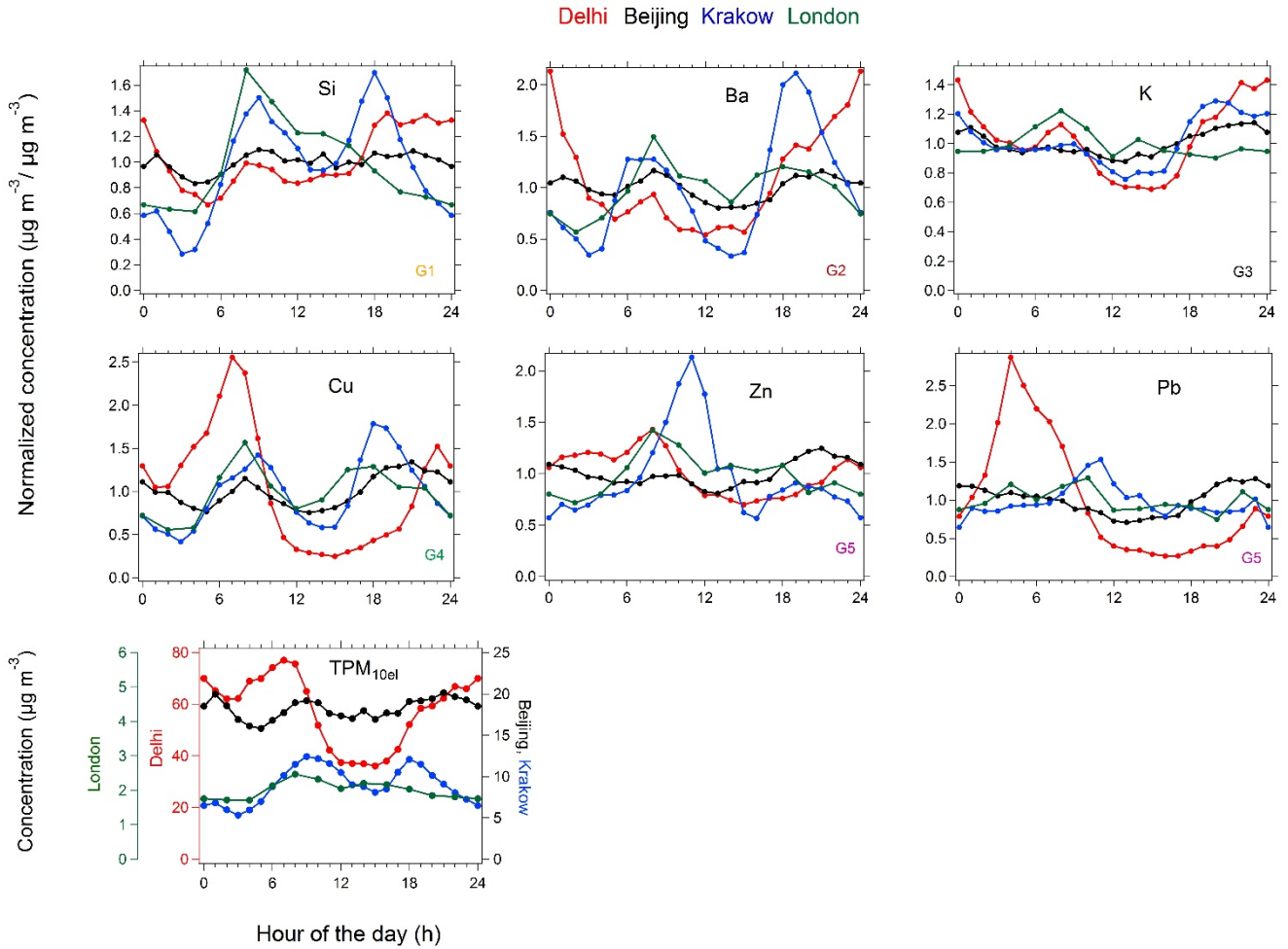
Figure 4: Diurnal patterns (means) of selected elements representative of each group (G1: Group 1, G2: Group 2, G3: Group 3, G4: Group 4, G5: Group 5) in PM$_{10}$ normalized by the mean values of the elements in PM$_{10}$, and the total elemental PM$_{10}$ (in µg m^{-3}, bottom) at all sites. Note that due to the time resolution of the original data the London data are 2-h averages, while the other data are 1-h averages.

18
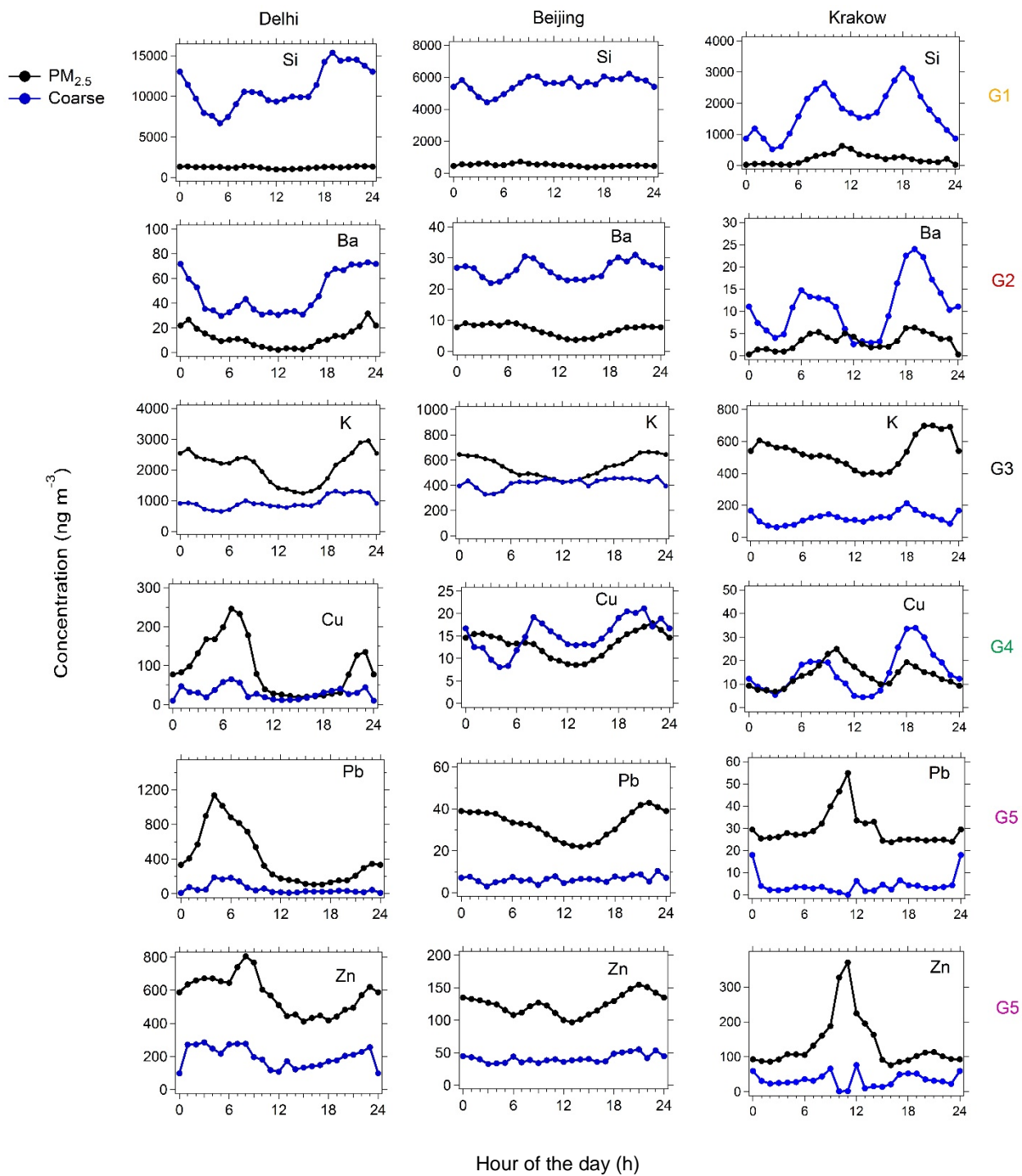
Figure 5: Diurnal variations of elements representative of each group (G1: Group 1, G2: Group 2, G3: Group 3, G4: Group 4, G5: Group 5) in PM$_{2.5}$ and coarse size fractions (PM$_{10}$–PM$_{2.5}$) at Delhi, Beijing, and Krakow (see Fig. S8 for London).